Journal of Neuroradiology 46 (2019) 52–60

Available online at ScienceDirect www.sciencedirect.com

Elsevier Masson France EM|consulte www.em-consulte.com

Original Article

Ipsilateral and contralateral cerebro-cerebellar white matter connections: A diffusion tensor imaging study in healthy adults

Efstratios Karavasilis[a,*,1], Foteini Christidi[b,1], Georgios Velonakis[a], Zoi Giavri[c], Nikolaos L. Kelekis[a], Efstathios P. Efstathopoulos[a], Ioannis Evdokimidis[b], Georges Dellatolas[d]

[a] Second Department of Radiology, University General Hospital "Attikon", Medical School, National and Kapodistrian University of Athens, Athens, Greece
[b] First Department of Neurology, Aeginiteion Hospital, Medical School, National and Kapodistrian University of Athens, Athens, Greece
[c] Department of Electrical and Computer Engineering, National Technical University of Athens, Athens, Greece
[d] Faculté de médecine UVSQ, Inserm, Université Paris-Saclay, 91190 Villejuif, France

ARTICLE INFO

Article history:
Available online 9 August 2018

Keywords:
Cerebellum
Cerebro-cerebellar
White matter
Diffusion tensor imaging
Tractography
Phantom

ABSTRACT

Background and purpose. – : The cerebellum has a pivotal role in regulating human behavior; yet whether this function is mediated only through contralateral cerebro-cerebellar pathways is under-investigated. Thus, we examined feed-backward and feed-forward ipsilateral and contralateral cerebro-cerebellar connections using a detereministic diffusion tensor imaging (DTI) algorithm, the robustness of which was also estimated using phantom DTI data.
Materials and methods. – : Fifty-one healthy controls (22–60 years old; 15 males/36 females) were scanned in a 3T MRI scanner with a 30-direction DTI sequence. Multiple region-of-interest (ROI) method was applied for the reconstruction of the ipsilateral and contralateral (based on cerebellar seed ROI) fronto-ponto-cerebellar (FPC), parieto-ponto-cerebellar (PPC), temporo-ponto-cerebellar (TPC), occipito-ponto-cerebellar (OPC) and dentate-rubro-thalamo-cortical (DRTC) tract bilaterally using the Brainance DTI Suite. A realistic diffusion MR phantom was used to evaluate the fiber tracking methodology for 16 fibers containing crossing, kissing, splitting and bending configurations.
Results. – Both contralateral and ipsilateral FPC, PPC, OPC and ipsilateral DRTC tracts were successfully reconstructed; the contralateral DRTC tract was not reconstructed in all subjects. Also, the TPC tract was not reproduced in several subjects mostly regarding the contralateral connection. Descriptive DTI measures (number of fibers, fractional anisotropy, radial and axial diffusivity) are presented for each tract. Regarding phantom data, Brainance DTI Suite returned a dataset of 16 fibers that almost perfectly matched the 16 ground truth fibers.
Conclusions. – We identified ipsilateral and contralateral connections using a clinically applicable DTI sequence, a robust deterministic algorithm and an unbiased methodology, which can be applied in daily practice in different brain pathologies.

Introduction

The cerebellum has strong connections with cortical and subcortical regions via white matter (WM) pathways [1]. Cerebellar WM tracts are categorized into spino-cerebellar, vestibulo-cerebellar and cerebro-cerebellar which connect the cerebellum with the spinal cord, the vestibular organs of the inner ear and the cerebrum, respectively. This paper focuses on the cerebro-cerebellar connections. The cerebellum receives input from the cerebrum via projections arising from the cortex and passing through the pontine nuclei and gives output to the cerebrum via projections arising from the dentate nucleus and passing through the thalamus [2,3]. Due to the absence of monosynaptic cerebro-cerebellar connections, classical histopathological tracing techniques were not able to identify the pathways between distinct cortical regions and specific cerebellar zones. However, the most advanced histopathological techniques have shown these connections but these findings concern in vitro and not in vivo studies [1].

Diffusion tensor imaging (DTI) is a widespread used in vivo tracking technique to study the integrity and the structural role of WM based on the water molecule brownian motion

* Corresponding author. 19 Papadiamantopoulou street, Athens, 11528, Greece.
E-mail address: stratoskaravasilis@yahoo.gr (E. Karavasilis).
[1] Shared first authorship.

https://doi.org/10.1016/j.neurad.2018.07.004
0150-9861/

and several DTI-derived quantitative metrics, including fractional anisotropy (FA), axial and radial diffusivity (AD and RD, respectively) [4,5]. Different DTI algorithms have been developed to mathematically identify the WM fibers of interest using deterministic and probabilistic models [6]. Probabilistic tractography models have been considered superior to deterministic ones in their ability to estimate fiber tracts since deterministic methods may underestimate the reconstruction of fibers in comparison to probabilistic tractography and dissection validation techniques [7]. However, robust deterministic algorithms have been recently implemented to more accurately calculate diffusion tensor parameters in voxels where fibers are likely to cross, thus overcoming not only the disadvantage of older deterministic algorithms but also time-consuming processes of probabilistic models [8,9]. The reconstruction of cerebro-cerebellar tracts using DTI tractography has considerable clinical significance. For instance, if these connections are mainly or exclusively contralateral, a cerebellar functional hemispheric asymmetry opposite to the cerebral functional hemispheric asymmetry could be expected, with verbal deficits after lesions of the right cerebellum and visuospatial deficits after lesions of the left cerebellum [1,2]. To our knowledge, only few studies so far have investigated the structural integrity of feed-forward and feed-backward cerebellar tracts in healthy population, mostly focusing on the contralateral connections [10–17] and much less the ipsilateral ones [18–22].

Thus, the aim of our study is to investigate the presence of feed-backward and feed-forward ipsilateral and contralateral connections between the cerebellum and the cerebrum using a detereministic DTI algorithm, the robustness of which is also estimated using a phantom experimental procedure.

Material and methods

Participants

We included 60 healthy control (HC) participants (22 males/38 females). Inclusion criteria were: age > 17 years old; right-handedness; Greek as native language. Exclusion criteria were: known contradictions to MRI; known or incidental abnormal findings in regular MRI; neurological or psychiatric disorders; developmental disorders including learning disabilities; major organic diseases including cardiovascular and metabolic pathologies; alcohol or drug abuse; psychotropic or other medication. Three participants did not undergo MRI due to claustrophobia and six were excluded due to the presence of motion artifacts. The mean age of the remaining 51 HC (15 males/36 females) was 37.69 ± 9.79 years old. All participants provided inform consent for the present study, which was approved by the local ethical committee and was conducted according to the 1964 Declaration of Helsinki and its later amendments.

MRI protocol

All participants underwent a whole-brain high resolution 3D–T1-weighted (HR_3DT1w) and 30-directional DTI protocol on a 3T Philips Achieva-Tx MR scanner (Philips, Best, The Netherlands) equipped with an eight-channel head coil. DTI acquisition included an axial single-shot spin-echo echo-planar imaging (EPI) sequence with 30 diffusion encoding directions and the following parameters: repetition time (TR): 7299 ms; echo time (TE): 68 ms; flip angle: 90°; field of view (FOV): 256×256 mm; acquisition voxel size: $2 \times 2 \times 2$ mm; sensitivity encoding reduction factor of 2; two b factors with 0 s/mm^2 (low b) and 1000 s/mm^2 (high b). Two numbers of excitations (NEX) were acquired per b value in order to ensure better signal-to-noise ratio. The acquisition consisted of 70 slices and the scan time was 8 min 40 s. All participants also received T2-fluid attenuation inversion recovery (T2-FLAIR) to exclude severe cerebrovascular disease according to standard neuroradiological criteria on visual inspection by an experienced neuroradiologist.

DTT analysis

DTT analysis was performed using the Brainance DTI Suite (Advantis Medical Imaging, Eindhoven, The Netherlands), with all DTI data sets having undergone motion and eddy-current correction with the registration tool available in the scanner and co-registration protocol with Brainance DTI suite before further analysis. We used region-of-interest (ROI) fiber tractography of the anatomical zone of the cortico-ponto-cerebellar tracts [i.e. fronto-ponto-cerebellar (FPC), parieto-ponto-cerebellar (PPC), occipito-ponto-cerebellar (OPC), and temporo-ponto-cerebellar (TPC)], and dentate-rubro-thalamo-cortical (DRTC) based on previously described protocols [13]. We used two ROIs for the reconstruction of cortico-ponto-cerebellar tracts (Supplementary Fig. 1) and the first ROI was placed in middle cerebellar peduncle which was defined at the coronal plane of the dorsal surface of the brainstem in Red-Green-Blue (RGB) color map. The second ROI was different for each cortico-ponto-cerebellar tract. Specifically: a) for the FPC, the second ROI was placed in the frontal lobe which was defined as anterior to the central sulcus at the axial plane just above the cingulated gyrus in the RGB color map; b) for the PPC, the second ROI was place in the parietal lobe which was defined as the region posterior to central sulcus at the axial plane just above the cingulated gyrus in the RGB color map; c) for the TPC, the second ROI was placed in the temporal lobe which was defined at the coronal plane of the anterior commissure in the RGB color map; d) for the OPC, the second ROI was placed in the occipital lobe at the coronal plane which was defined as posterior to the corpus callosum and inferior to the parieto-occipital sulcus. For the reconstruction of the DRTC (Supplementary Fig. 2), the first ROI was placed in the dentate nucleus, which was defined at the level of the pontomedullary junction whereas the second ROI was placed in the red nucleus axially at the level of the cerebral peduncly in the pons. Both ROIs for the DRTC were placed in a b0 DWI image. Since we reconstructed both contralateral and ipsilateral tracts using the appropriate predefined ROIs, the second ROI for all cortico-ponto-cerebellar tracts and the DRTC was placed either contralaterally or ipsilaterally to the first ROI. To reconstruct the tracts we used the following DTI thresholds: fractional anisotropy (FA) = 0.15; angle = 70°; step size = 1. Number of fibers (NoF), FA, axial diffusivity (AD) and radial diffusivity (RD) DTI metrics were automatically extracted for each tract and represent the average FA, AD and RD value along the tract. Descriptive measures were obtained for all DTI data.

Realistic DTI phantom protocol and analysis

For the assessment of the fiber tracking methodology implemented in Brainance DTI suite (Advantis Medical Imaging, Eindhoven, The Netherlands) a realistic diffusion MR phantom was used, containing numerous crossing, kissing, splitting and bending configurations that were purposely developed to this end [23] as shown in the Fig. 1a–b. The angles between crossing fibers were carefully determined, although not used during evaluation [24]. Diffusion-weighted data of the phantom were acquired on the 3T Tim Trio MRI systems of the NeuroSpin centre. A single-shot diffusion-weighted twice refocused spin-echo echo-planar pulse sequence was used to perform the acquisition, while compensating the eddy-current to the first order. The parameters for

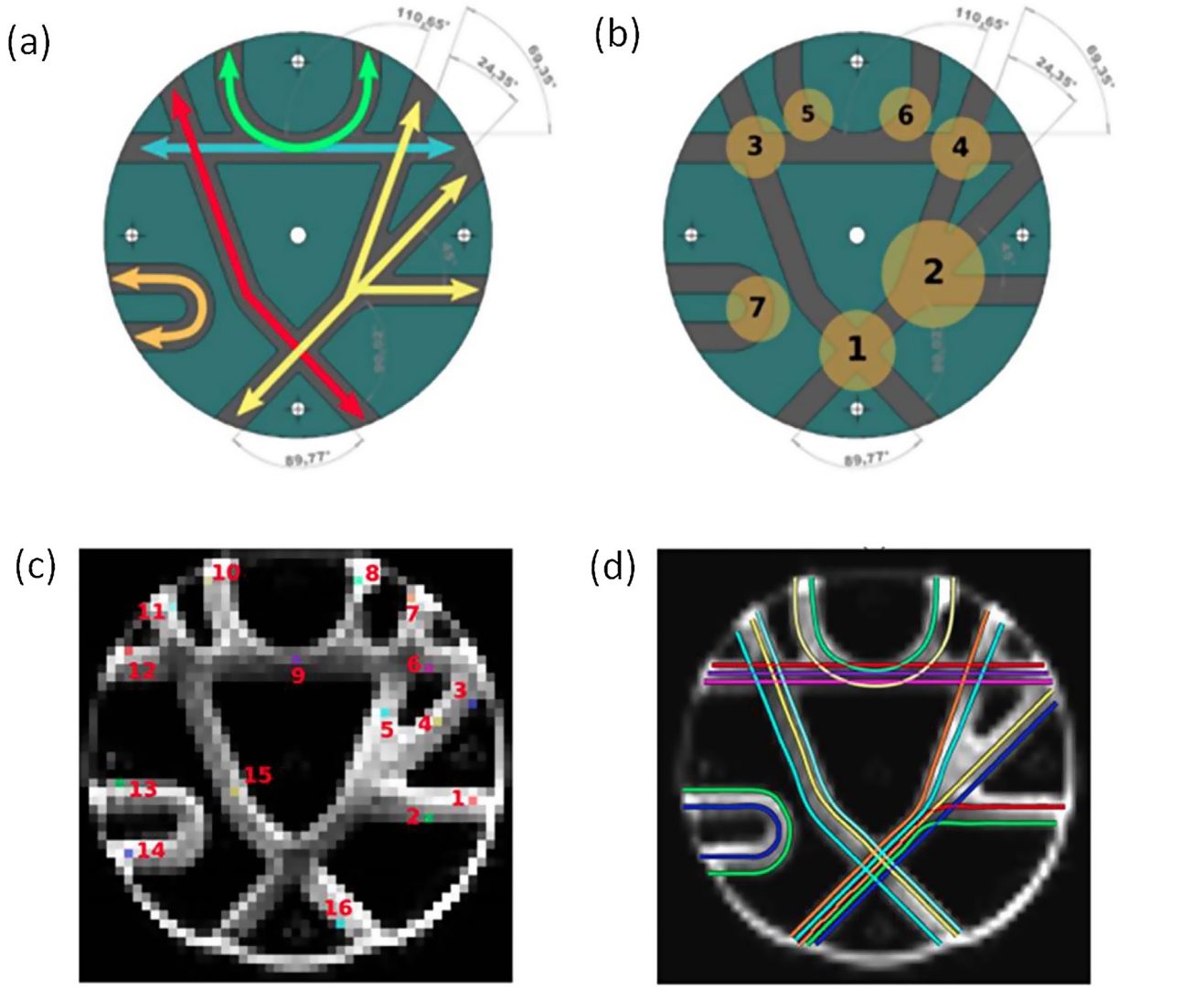

Fig. 1. Phantom design and ground truth fibers. a: the phantom design that mimics a coronal section of the human brain, with fiber pathways being highlighted in colors and arrows indicating the directions of the synthetic fiber bundles; b: various crossing, splitting and kissing fiber configurations are numbered for a fast text referencing; c: the 16 seed voxels defined on the $3 \times 3 \times 3$ mm dataset; d: the ground truth fibers on a B0 image.

the acquisition were as follows: FOV: 192×192 mm; acquisition voxel size: $3 \times 3 \times 3$ mm; partial Fourier factor 6/8, parallel reduction factor of 2; TR: 5000 ms; 2 repetitions. Diffusion sensitization at b value b = 650 s/mm^2 corresponding to the TE: 77 ms. Three slices were acquired. The diffusion sensitization was applied along a set of 64 orientations uniformly distributed over the sphere. All DTI pre- and post-processing was done using Brainance DTI Suite (Advantis Medical Imaging, Eindhoven, The Netherlands). To facilitate the evaluation of the results, the analysis was restricted to a set of 16 fibers traversing 16 manually identified voxels, or seeds. The choice of those 16 spatial positions was made to ensure that a single fiber bundle passes through each of them to avoid ambiguity on the result and to facilitate the evaluation. Comparison of an undetermined number of fibers to the ground truth, whose number of bundles per voxel is precisely known, is non-trivial. Consequently, seeds were defined in voxels where a unique fiber bundle is expected and the ask was to return a single representative fiber of the bundle traversing each seed voxel. The 16 seeds, labeled from 1 to 16, are shown in the Fig. 1c–d.

Results

DTI in healthy participants: reconstruction and descriptive measures for cerebro-cerebellar tracts

Both contralateral and ipsilateral FPC (Fig. 2), PPC (Fig. 3), OPC (Fig. 4) and ipsilateral DRTC (Fig. 5) tracts were successfully reconstructed for all participants; the contralateral DRTC tracts were not reconstructed in 20 (seed: right cerebellum) and 29 (seed: left cerebellum) out of 51 subjects. Furthermore, the TPC tract (Fig. 6) was not reproduced in several subjects mostly regarding the contralateral connection as it is shown in Table 1. For each tract, we extracted DTI metrics and all descriptive measures (NoF, FA, AD, RD) are presented in Table 1.

DTI in Phantom: validation of fiber reconstruction

Evaluation of the fiber tracking results was performed on a per-fiber basis. Thus, the candidate fiber passing through seed N can be compared to the ground truth fiber going through the same seed.

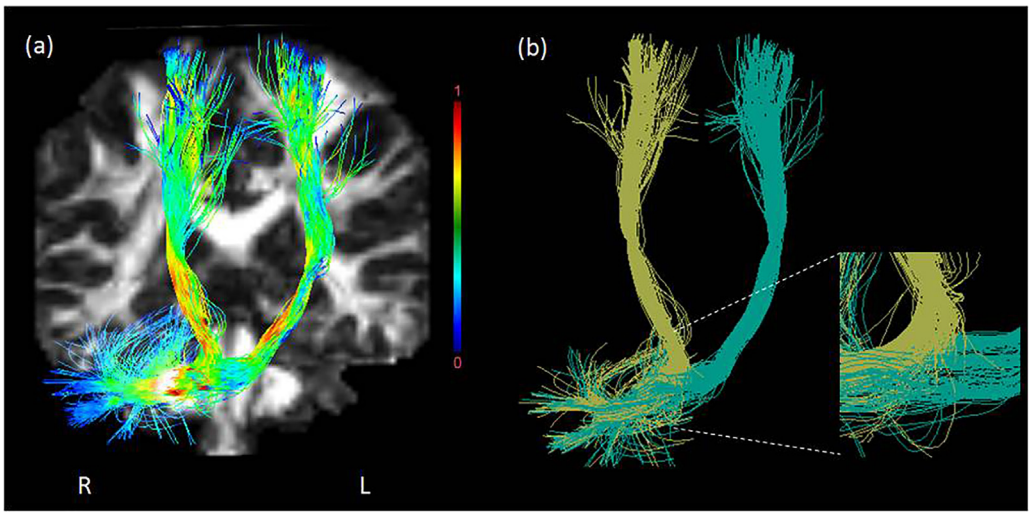

Fig. 2. Reconstruction of ipsilateral and contralateral fronto-ponto-cerebellar tract (FPC) with right cerebellar seed region-of-interest (ROI) depicted in (a) fractional anisotropy (FA) color code and overlaid onto a coronal FA map and (b) conventional colors (yellow: ipsilateral FPC; turquoise: contralateral FPC) with crossing fibers being separately visualized at the zoomed-in lower panel.

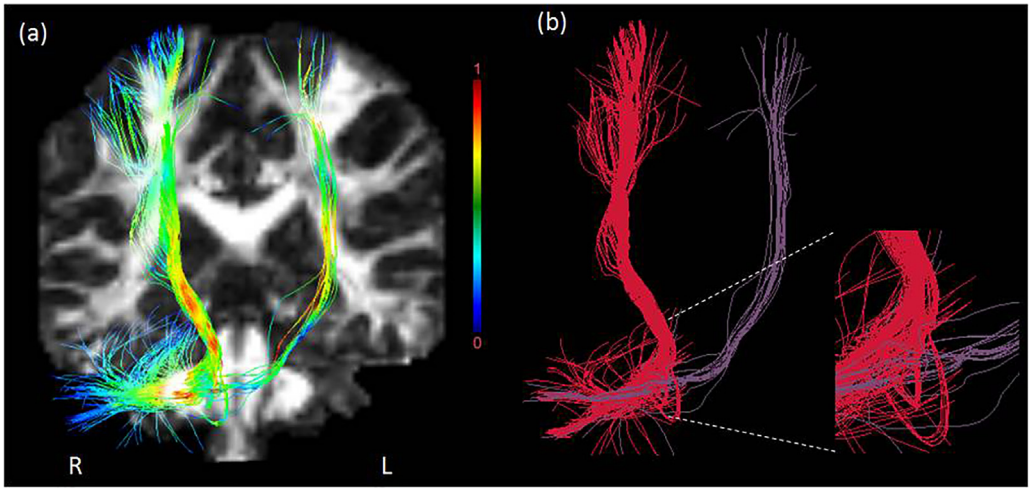

Fig. 3. Reconstruction of ipsilateral and contralateral PPC tract with right cerebellar seed region-of-interest (ROI) depicted in (a) fractional anisotropy (FA)color code and overlaid onto a coronal FA map and (b) conventional colors (red: ipsilateral PPC; purple: contralateral PPC) with crossing fibers being separately visualized at the zoomed-in lower panel.

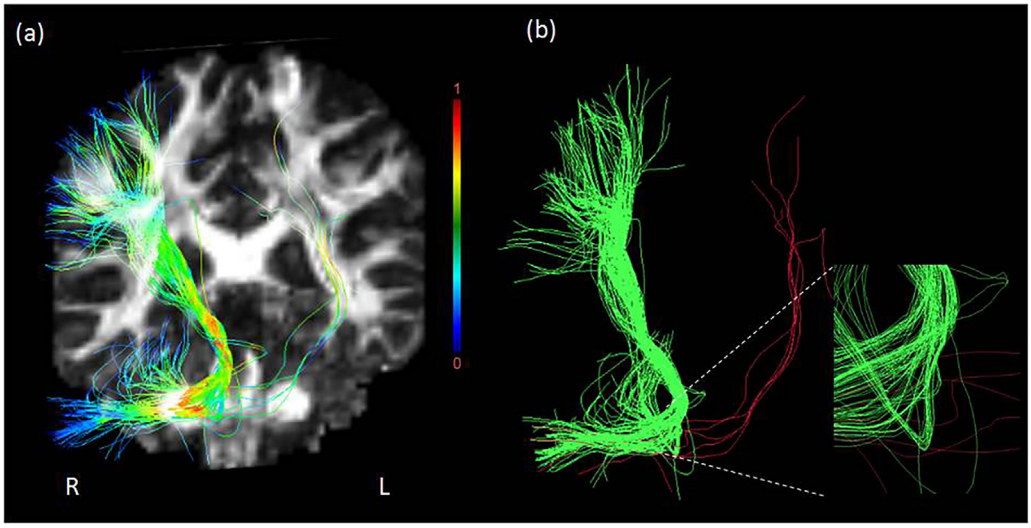

Fig. 4. Reconstruction of ipsilateral and contralateral OPC tract with right cerebellar seed region-of-interest (ROI) depicted in (a) fractional anisotropy (FA) color code and overlaid onto a coronal FA map and (b) conventional colors (green: ipsilateral OPC; red: contralateral OPC) with crossing fibers being separately visualized at the zoomed-in lower panel.

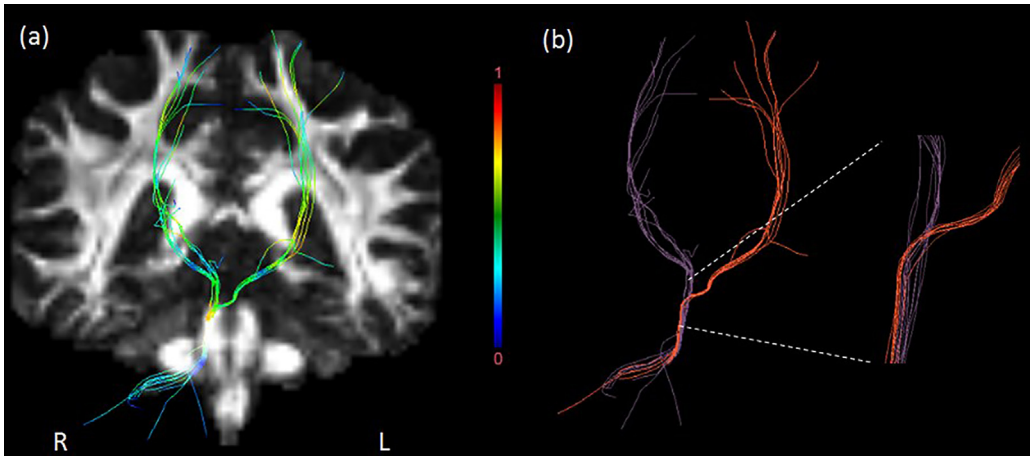

Fig. 5. Reconstruction of ipsilateral and contralateral TPC tract with right cerebellar seed region-of-interest (ROI) depicted in (a) fractional anisotropy (FA) color code and overlaid onto a coronal FA map and (b) conventional colors (purple: ipsilateral TPC; blue: contralateral TPC).

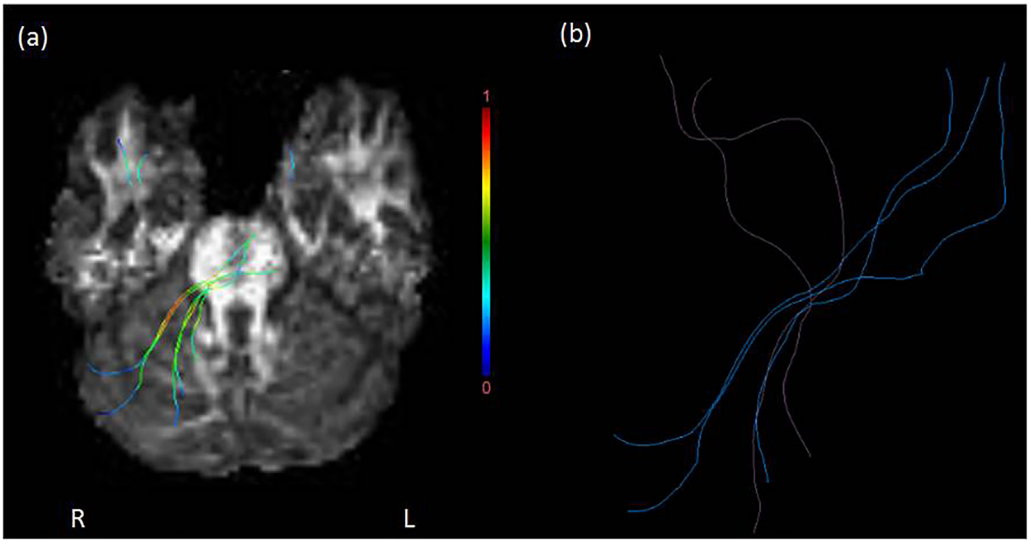

Fig. 6. Reconstruction of ipsilateral and contralateral DRTC tract with right cerebellar seed ROI depicted in (a) fractional anisotropy (FA) color code and overlaid onto a coronal FA map and (b) conventional colors (purple: ipsilateral DRTC; orange: contralateral DRTC).

Consequently, the evaluation methodology narrows down to the evaluation of differences between pairs of curves. Brainance DTI Suite returned a dataset composed of 16 fibers that almost perfectly matched the 16 ground truth fibers [24] as shown in Fig. 7.

Discussion

Considering the pivotal role of cerebellum in regulating both motor and cognitive/affective aspects of human behavior [1,2], we herein examined the anatomical connections between the cerebellum and the cerebrum using in vivo DTI tractography and focusing on feed-forward and feed-backward cerebellar pathways. By applying an unbiased approach we have identified both contralateral and ipsilateral tracts, which cannot be considered false-positive findings due to the current robust deterministic algorithm since phantom data analysis verified the above results.

DRTC is traditionally described as the only feed-forward cerebellar tract passing from the cerebellar nuclei and dentate nucleus, arriving at the superior cerebellar peduncle, red nucleus, thalamus and finally terminating at the cerebral cortex [25–27]. Previous studies referred almost exclusively to contralateral connections disregarding ipsilateral ones. Crossed cerebro-cerebellar atrophy via the degeneration of the dentate nucleus has been attributed to long-standing lesions of the contralateral hemisphere [28]. Histopathological research in mammals has also provided evidence for such connections based on the site of cerebellar injection and the labeled neurons in the contralateral hemisphere [29,30]. In addition, DTI studies identified the contralateral connections of DRTC tract using probabilistic tractography [14,15]. However, using the same method Habas and Cabanis [20] reconstructed only the ipsilateral bundles, while Keser et al. [13] considered a priori feed-forward projections as ipsilateral connection using deterministic algorithm. Yet there is no evidence so far to assess only ipsilateral or contralateral connections. Therefore, using a robust deterministic algorithm to conquer the limitation of crossing and kissing fibers, we regarded and reconstructed ipsilateral and contralateral connections of DRTC, which are in line with tractography combined with micro-dissection [25]. The failure of reconstruction of contralateral bundles in some cases could be resulted from the termination of tracts prior to cerebral cortex, in accordance with historical tracing literature [31].

Similarly to feed-forward connections (i.e. DRTC), we examined and reconstructed contralateral and ipsilateral connections between the cerebellum and the cerebral lobes (i.e. FPC, TPC, PPC, OPC). Nevertheless, post-mortem histopathological and in vivo DTI studies mainly refer to the presence of contralateral connections

Table 1
Number of subjects with successfully reconstructed cortico-cerebellar tracts and DTI metrics for each tract.

Tract	Seed: right cerebellum		Seed: left cerebellum	
	Contralateral	Ipsilateral	Contralateral	Ipsilateral
FPC	51/51	51/51	51/51	51/51
NoF	131.04 ± 88.14	203.94 ± 140.92	179.84 ± 85.10	170.69 ± 111.39
FA	0.49 ± 0.02	0.49 ± 0.02	0.50 ± 0.01	0.50 ± 0.02
AD	$1.08 \times 10^{-02} \pm 6.86 \times 10^{-02}$	$1.16 \times 10^{-03} \pm 2.29 \times 10^{-05}$	$1.19 \times 10^{-03} \pm 3.05 \times 10^{-05}$	$1.16 \times 10^{-03} \pm 2.65 \times 10^{-05}$
RD	$5.06 \times 10^{-04} \pm 1.88 \times 10^{-05}$	$5.09 \times 10^{-04} \pm 1.61 \times 10^{-05}$	$5.09 \times 10^{-04} \pm 1.81 \times 10^{-05}$	$4.91 \times 10^{-04} \pm 1.99 \times 10^{-05}$
PPC	51/51	51/51	51/51	51/51
NoF	36.33 ± 37.43	129.65 ± 79.24	62.37 ± 57.22	91.51 ± 63.88
FA	0.49 ± 0.02	0.49 ± 0.02	0.50 ± 0.02	0.50 ± 0.02
AD	$1.19 \times 10^{-03} \pm 4.30 \times 10^{-05}$	$1.20 \times 10^{-03} \pm 2.64 \times 10^{-05}$	$1.22 \times 10^{-03} \pm 4.22 \times 10^{-05}$	$1.19 \times 10^{-03} \pm 2.53 \times 10^{-05}$
RD	$5.22 \times 10^{-04} \pm 2.79 \times 10^{-05}$	$5.25 \times 10^{-04} \pm 2.05 \times 10^{-05}$	$5.25 \times 10^{-04} \pm 2.39 \times 10^{-05}$	$5.04 \times 10^{-04} \pm 5.27 \times 10^{-05}$
TPC	18/51	35/51	8/51	44/51
NoF	0.63 ± 1.06	2.82 ± 4.91	0.33 ± 0.95	3.31 ± 3.55
FA	0.43 ± 0.03	0.41 ± 0.02	0.42 ± 0.02	0.43 ± 0.03
AD	$1.16 \times 10^{-03} \pm 4.93 \times 10^{-05}$	$1.18 \times 10^{-03} \pm 5.61 \times 10^{-05}$	$1.16 \times 10^{-03} \pm 1.01 \times 10^{-04}$	$1.18 \times 10^{-03} \pm 5.03 \times 10^{-05}$
RD	$5.75 \times 10^{-04} \pm 4.40 \times 10^{-05}$	$6.07 \times 10^{-04} \pm 3.40 \times 10^{-05}$	$5.98 \times 10^{-04} \pm 6.31 \times 10^{-05}$	$5.91 \times 10^{-04} \pm 4.09 \times 10^{-05}$
OPC	51/51	51/51	51/51	51/51
NoF	23.80 ± 23.23	76.94 ± 61.15	28.88 ± 38.17	103.82 ± 95.10
FA	0.48 ± 0.02	0.47 ± 0.02	0.48 ± 0.02	0.49 ± 0.02
AD	$1.22 \times 10^{-03} \pm 5.20 \times 10^{-05}$	$1.20 \times 10^{-03} \pm 3.42 \times 10^{-05}$	$1.22 \times 10^{-03} \pm 4.62 \times 10^{-05}$	$1.21 \times 10^{-03} \pm 3.02 \times 10^{-05}$
RD	$5.44 \times 10^{-04} \pm 3.08 \times 10^{-05}$	$5.46 \times 10^{-04} \pm 2.59 \times 10^{-05}$	$5.46 \times 10^{-04} \pm 3.50 \times 10^{-05}$	$5.28 \times 10^{-04} \pm 2.42 \times 10^{-05}$
DRTC	31/51	51/51	22/51	51/51
NoF	4.37 ± 7.12	33.12 ± 29.54	1.61 ± 3.31	25.98 ± 21.26
FA	0.44 ± 0.02	0.43 ± 0.02	0.43 ± 0.04	0.44 ± 0.02
AD	$1.15 \times 10^{-03} \pm 6.17 \times 10^{-05}$	$1.21 \times 10^{-03} \pm 5.31 \times 10^{-05}$	$1.17 \times 10^{-03} \pm 4.34 \times 10^{-05}$	$1.18 \times 10^{-03} \pm 4.51 \times 10^{-05}$
RD	$5.59 \times 10^{-04} \pm 3.78 \times 10^{-05}$	$6.01 \times 10^{-04} \pm 4.67 \times 10^{-05}$	$5.75 \times 10^{-04} \pm 4.86 \times 10^{-05}$	$5.72 \times 10^{-04} \pm 3.16 \times 10^{-05}$

FA, AD and RD values were extracted with missing values for cases where tracts were not successfully reconstructed. DTI: diffusion tensor imaging; NoF: number of fibers; FPC: fronto-ponto-cerebellar tract; PPC: parieto-ponto-cerebellar tract; TPC: temporo-ponto-cerebellar tract; OPC: occipito-ponto-cerebellar tract; DRTC: dentate-rubro-thalamo-cortical tract; FA: fractional anisotropy; AD: axial diffusivity; RD: radial diffusivity.

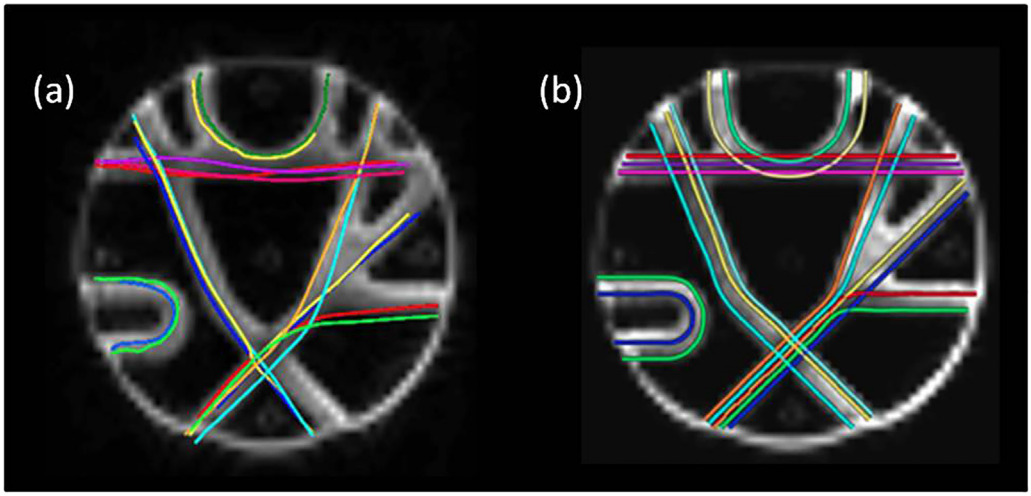

Fig. 7. (a) The 16 fiber trajectories that were computed on the $3 \times 3 \times 3$ mm phantom dataset and (b) the ground truth fibers.

in cortico-ponto-cellebelar tracts [12,32,33]. Only a handful of DTI studies supported the presence of ipsilateral cerebro-cerebellar connections [18–20,34] with all of them not relying on clinically-used deterministic algorithms but on probabilistic ones. It is must be noted that using advanced acquisition and post-processing methodology, i.e. high-angular resolution diffusion imaging and probabilistic tractography, Palesi and colleagues [35] assessed the connectivity between the cerebrum and cerebellar cortex and delineated both ipsilateral and contralateral pathways when cerebral target ROIs were not included and only cerebellar seed ROIs were considered in the DTI analysis. Also, using similar imaging protocol and post-processing analysis Pieterman and colleagues [16] recognized ipsilateral and contralateral pathways in infants. The lack of knowledge about the presence of ipsilateral pathways led the latter to be considered as "artifacts secondary to interference by the large white matter tracts converging on the brainstem from other circuits" [34] due to kissing fibers in studies where ipsilateral connections were identified [36].

An intriguing point in the cerebellar connectivity literature remains its connection with temporal structures. The functional connectivity between the cerebellum and the temporal lobes has been shown via fMRI [37–41] and electrophysiological/lesion studies [42]. The above-mentioned findings may imply the presence of temporo-cerebellar structural connectivity; yet some DTI studies failed to consistently identify these tracts in all subjects due the high track curvature and various intersections [3,13,43]. Our results confirm the existence of temporo-cerebellar structural pathways at least in some subjects and mainly with regards to the ipsilateral connections. In the rest of the subjects, we failed to reconstruct the TPC even by applying different angular thresholds. Thus, the iden-

tification of TPC tract could be considered questionable based on available clinical or commonly used research DTI scanning protocols and fiber tracking algorithms.

From a methodological point of view, the application of the same tractography protocol in high- and ultra-high resolution DTI data might further advance our knowledge not only regarding the TPC but also other cortico-ponto-cerebellar connections of high complexity, such as the DRTC. The simple diffusion tensor model has been considered less appropriate to characterize complex fiber architecture [44,45]. There is no doubt that the implementation of methodological advances in diffusion MRI, such as the high-angular resolution diffusion imaging (HARDI) protocol [46] or diffusion spectrum MRI (DSI) protocol [47], along with the use of fMRI – dMRI techniques [48–51] can definitely offer valuable insights into the structural cortico-cerebellar connectivity and its functional correlates. However, the above-mentioned protocols are not easily applied in everyday clinical practice not only because of available scanner features but also prolonged scanning time [46] which further increases the possibility of participant- and system-related artifacts (e.g. due to head motion and gradient-related, respectively).

We can assume the reliability of our findings based on the following:

- we included an adequate sample size for the descriptive purposes of the present study and used a robust DTI algorithm which has been previously shown to be reliable for the reconstruction of WM pathways including fibers (e.g. lateral cortical projections and crossing pontine fibers of the corticospinal tract) that cannot be depicted with similar deterministic algorithms [9];
- we further confirmed the reliability of reconstructed crossing, kissing and bending fibers by herein evaluating the robustness of the algorithm with a phantom DTI dataset that clearly provided similar findings between the ground truth and Brainance reconstructed fibers;
- evidence from probabilistic DTI studies highlights the presence of ipsilateral cerebro-cerebellar connections which are more likely to be attributed to possible false-positive fibers though;
- evidence from cerebellar lesion studies in children and adults does not always support the presence of a cerebellar hemispheric functional asymmetry opposite to the cerebral hemispheric functional asymmetry (although some clinical studies reported verbal deficits in lesions of the right cerebellum and visuospatial deficits in lesion of the left cerebellum [52–54], many other did not confirm this finding [55–57]);
- although ex vivo animal studies with or without simultaneous in vivo examination of WM is highly applied and valuable for the comprehension of the pattern of WM connections, transferring knowledge acquired from animal research to the study of human brain may yield inconclusive findings or even guide researchers to a priori assumptions and not unbiased examination of human brain connections.

Both the use of a DTI sequence, which is applicable in clinical practice and the majority of MRI scanners and the post-processing analysis with software that overcomes the time-consuming procedures of the probabilistic analysis constitute a significant advantage of our study and needs further evaluation in clinical samples with profound or salient cerebellar-related cognitive-behavioral impairment.

Despite the previous strengths, our study is not without caveats. First of all, we used the conventional anatomical terms of "afferent vs. efferent" projections although DTI inherently lacks the ability to visualize fibers' orientation. In addition, we do acknowledge the large deviation in the number of fibers within each tract. However significant deviations in number of fibers have been reported in bundles with lower or higher complexity with regards to the curvature [58,59]. Our intention was to identify cerebro-cerebellar connections with an unbiased approach which is methodological plausible and reliable, without in-depth analysis and discussion of the anatomical trajectories of the reconstructed tracts. The lack of functional and/or behavioral data is another limitation of the study, which did not allow us to comparatively study the structural and functional cerebro-cerebellar connections and is part of another ongoing study of our laboratory. In addition we did not apply correction of EPI induced distortions, such as geometric distortion caused B0 inhomogeneity, which is often applied to successfully reduce EPI distortions and improve the quality of DTI-derived quantities and thus the anatomical fidelity of DTI [60–63]. Most pronounced artifacts, which are usually more severe at higher magnetic field strengths, are observed in air-tissue interplaces, such as the ventral portions of the fronto-temporal regions and specifically near the sphenoid sinus and the temporal petrous bone. Thus, we have to take into consideration the above in relation to the failure of TPC or DRTC reconstruction. Furthermore, with regards to the phantom DTI analysis, we should acknowledge that several phantoms that are commonly used in MRI routine practice do not represent the best option for DWI/DTI images [64]. In the present study, we used public-available data from a realist diffusion MR phantom containing numerous crossing, kissing, splitting and bending configurations [24] in order to examine the evaluate the robustness of the fiber tracking algorithm implemented in Brainance DTI suite; yet we should highlight that even new diffusion phantoms dedicated to the study and validation of advanced models, including HARDI models [23], might not address the issue of the complexity of human brain architecture. Finally, we do acknowledge the inherent limitations of ROI-based tractography [65], yet all data were post-processed by an experienced user.

Conclusion

We identified both ipsilateral and contralateral connections using a clinically applicable DTI sequence, a robust deterministic algorithm and an unbiased methodology that can be applied in daily practice in clinical protocols. The combination of clinical and experimental results might provide a plausible explanation for the previous inconsistent findings, which have provoked confusion regarding the presence of ipsilateral and contralateral cerebellar connections and have been explained as part of DTI-related artifacts (i.e. kissing fibers) or researchers' a priori approach towards unilateral connections.

Disclosure of interest

The authors declare that they have no competing interest.

Acknowledgements

Part of this study was presented as e-poster in the 5th International Congress on Neurobiology, Psychopharmacology & Treatment Guidance (25–28 May, 2017, Chalkidiki, Greece) and thus we would like to thank all attendees for their constructive comments. Finally, we would like to thank all the healthy controls for their willingness to participate in the present study.

Appendix A. Supplementary data

Supplementary material related to this article can be found, in the online version, at https://doi.org/10.1016/j.neurad.2018.07.004.

References

[1] Buckner RL. The cerebellum and cognitive function: 25 years of insight from anatomy and neuroimaging. Neuron 2013;80(3):807–15.
[2] Schmahmann JD, Pandya DN. Disconnection syndromes of basal ganglia, thalamus, and cerebro-cerebellar systems. Cortex 2008;44(8):1037–66.
[3] Ramnani N. The primate cortico-cerebellar system: anatomy and function. Nat Rev Neurosci 2006;7(7):511–22.
[4] Alexander AL, Lee JE, Lazar M, Field AS. Diffusion tensor imaging of the brain. Neurotherapeutics 2007;4(3):316–29.
[5] Mori S, Zhang J. Principles of diffusion tensor imaging and its applications to basic neuroscience research. Neuron 2006;51(5):527–39.
[6] Nucifora PG, Verma R, Lee SK, Melhem ER. Diffusion tensor MR imaging and tractography: exploring brain microstructure and connectivity. Radiology 2007;245(2):367–84.
[7] Iglesias JE, Thompson PM, Liu CY, Tu Z. Fast approximate stochastic tractography. Neuroinformatics 2012;10(1):5–17.
[8] Qazi AA, Radmanesh A, O'Donnell L, Kindlmann G, Peled S, Whalen S, et al. Resolving crossings in the corticospinal tract by two-tensor streamline tractography: method and clinical assessment using fMRI. NeuroImage 2009;47(Suppl. 2):T98–106.
[9] Christidi F, Karavasilis E, Samiotis K, Bisdas S, Papanikolaou N. Fiber tracking: A qualitative and quantitative comparison between four different software tools on the reconstruction of major white matter tracts. Eur J Radiol 2016;3:153–61.
[10] Catani M, Jones DK, Daly E, Embiricos N, Deeley Q, Pugliese L, et al. Altered cerebellar feedback projections in Asperger syndrome. NeuroImage 2008;41(4):1184–91.
[11] Granziera C, Schmahmann JD, Hadjikhani N, Meyer H, Meuli R, Wedeen V, et al. Diffusion spectrum imaging shows the structural basis of functional cerebellar circuits in the human cerebellum in vivo. PloS One 2009;4(4):e5101.
[12] Kamali A, Kramer LA, Frye RE, Butler IJ, Hasan KM. Diffusion tensor tractography of the human brain cortico-ponto-cerebellar pathways: a quantitative preliminary study. J Magn Reson Imaging 2010;32(4):809–17.
[13] Keser Z, Hasan KM, Mwangi BI, Kamali A, Ucisik-Keser FE, Riascos RF, et al. Diffusion tensor imaging of the human cerebellar pathways and their interplay with cerebral macrostructure. Front Neuroanat 2015;9:41.
[14] Kwon HG, Hong JH, Hong CP, Lee DH, Ahn SH, Jang SH. Dentatorubrothalamic tract in human brain: diffusion tensor tractography study. Neuroradiology 2011;53(10):787–91.
[15] Pelzer EA, Hintzen A, Goldau M, von Cramon DY, Timmermann L, Tittgemeyer M. Cerebellar networks with basal ganglia: feasibility for tracking cerebellopallidal and subthalamo-cerebellar projections in the human brain. Eur J Neurosci 2013;38(8):3106–14.
[16] Pieterman K, Batalle D, Dudink J, Tournier JD, Hughes EJ, Barnett M, et al. Cerebello-cerebral connectivity in the developing brain. Brain Struct Funct 2017;222(4):1625–34.
[17] van Baarsen KM, Kleinnijenhuis M, Jbabdi S, Sotiropoulos SN, Grotenhuis JA, van Cappellen van Walsum AM. A probabilistic atlas of the cerebellar white matter. NeuroImage 2016;124(Pt A):724–32.
[18] Doron KW, Funk CM, Glickstein M. Fronto-cerebellar circuits and eye movement control: a diffusion imaging tractography study of human cortico-pontine projections. Brain Res 2010;1307:63–71.
[19] Habas C, Cabanis EA. Cortical projection to the human red nucleus: complementary results with probabilistic tractography at 3T. Neuroradiology 2007;49(9):777–84.
[20] Habas C, Cabanis EA. Anatomical parcellation of the brainstem and cerebellar white matter: a preliminary probabilistic tractography study at 3T. Neuroradiology 2007;49(10):849–63.
[21] Jissendi P, Baudry S, Baleriaux D. Diffusion tensor imaging (DTI) and tractography of the cerebellar projections to prefrontal and posterior parietal cortices: a study at 3T. J Neuroradiol 2008;35(1):42–50.
[22] Salamon N, Sicotte N, Drain A, Frew A, Alger JR, Jen J, et al. White matter fiber tractography and color mapping of the normal human cerebellum with diffusion tensor imaging. J Neuroradiol 2007;34(2):115–28.
[23] Poupon C, Rieul B, Kezele I, Perrin M, Poupon F, Mangin JF. New diffusion phantoms dedicated to the study and validation of high-angular-resolution diffusion imaging (HARDI) models. Magn Reson Med 2008;60(6):1276–83.
[24] Fillard P, Descoteaux M, Goh A, Gouttard S, Jeurissen B, Malcolm J, et al. Quantitative evaluation of 10 tractography algorithms on a realistic diffusion MR phantom. NeuroImage 2011;56(1):220–34.
[25] Meola A, Yeh FC, Fellows-Mayle W, Weed J, Fernandez-Miranda JC. Human connectome-based tractographic atlas of the brainstem connections and surgical approaches. Neurosurgery 2016;79(3):437–55.
[26] Oishi K, Crain B. MRI atlas of human white matter. 2nd ed. Amsterdam: Elsevier/Academic Press; 2011. [vii, 257 pages].
[27] Snell RS. Clinical neuroanatomy. 7th ed. Philadelphia, Pa.: Wolters Kluwer Health/Lippincott Williams & Wilkins; 2010. [542 S. p.].
[28] Glickstein M, Sultan F, Voogd J. Functional localization in the cerebellum. Cortex 2011;47(1):59–80.
[29] Kelly RM, Strick PL. Cerebellar loops with motor cortex and prefrontal cortex of a nonhuman primate. J Neurosci 2003;23(23):8432–44.
[30] Middleton FA, Strick PL. Cerebellar projections to the prefrontal cortex of the primate. J Neurosci 2001;21(2):700–12.
[31] Brodal A. Neurological anatomy in relation to clinical medicine. Third ed. New York: Oxford University Press; 1981. [1053 S. p.].
[32] Schmahmann JD, Rosene DL, Pandya DN. Ataxia after pontine stroke: insights from pontocerebellar fibers in monkey. Ann Neurol 2004;55(4):585–9.
[33] Voogd J, Glickstein M. The anatomy of the cerebellum. Trends Neurosci 1998;21(9):370–5.
[34] Hyam JA, Owen SL, Kringelbach ML, Jenkinson N, Stein JF, Green AL, et al. Contrasting connectivity of the ventralis intermedius and ventralis oralis posterior nuclei of the motor thalamus demonstrated by probabilistic tractography. Neurosurgery 2012;70(1):162–9 [discussion 9].
[35] Palesi F, Tournier JD, Calamante F, Muhlert N, Castellazzi G, Chard D, et al. Contralateral cerebello-thalamo-cortical pathways with prominent involvement of associative areas in humans in vivo. Brain Struct Funct 2015;220(6):3369–84.
[36] Abdul-Kareem IA, Stancak A, Parkes LM, Al-Ameen M, Alghamdi J, Aldhafeeri FM, et al. Plasticity of the superior and middle cerebellar peduncles in musicians revealed by quantitative analysis of volume and number of streamlines based on diffusion tensor tractography. Cerebellum 2011;10(3):611–23.
[37] Buckner RL, Krienen FM, Castellanos A, Diaz JC, Yeo BT. The organization of the human cerebellum estimated by intrinsic functional connectivity. J Neurophysiol 2011;106(5):2322–45.
[38] Dobromyslin VI, Salat DH, Fortier CB, Leritz EC, Beckmann CF, Milberg WP, et al. Distinct functional networks within the cerebellum and their relation to cortical systems assessed with independent component analysis. NeuroImage 2012;60(4):2073–85.
[39] Habas C, Guillevin R, Abanou A. Functional connectivity of the superior human temporal sulcus in the brain resting state at 3T. Neuroradiology 2011;53(2):129–40.
[40] Krienen FM, Buckner RL. Segregated fronto-cerebellar circuits revealed by intrinsic functional connectivity. Cereb Cortex 2009;19(10):2485–97.
[41] O'Reilly JX, Beckmann CF, Tomassini V, Ramnani N, Johansen-Berg H. Distinct and overlapping functional zones in the cerebellum defined by resting state functional connectivity. Cereb Cortex 2010;20(4):953–65.
[42] Snider RS, Maiti A. Cerebellar contributions to the Papez circuit. J Neurosci Res 1976;2(2):133–46.
[43] Sokolov AA, Erb M, Grodd W, Pavlova MA. Structural loop between the cerebellum and the superior temporal sulcus: evidence from diffusion tensor imaging. Cereb Cortex 2014;24(3):626–32.
[44] Vos SB, Jones DK, Jeurissen B, Viergever MA, Leemans A. The influence of complex white matter architecture on the mean diffusivity in diffusion tensor MRI of the human brain. NeuroImage 2012;59(3):2208–16.
[45] De Santis S, Drakesmith M, Bells S, Assaf Y, Jones DK. Why diffusion tensor MRI does well only some of the time: variance and covariance of white matter tissue microstructure attributes in the living human brain. NeuroImage 2014;89:35–44.
[46] Mori S. Introduction to diffusion tensor imaging. Amsterdam: Elsevier; 2007. [176 S. p.].
[47] Wedeen VJ, Wang RP, Schmahmann JD, Benner T, Tseng WY, Dai G, et al. Diffusion spectrum magnetic resonance imaging (DSI) tractography of crossing fibers. NeuroImage 2008;41(4):1267–77.
[48] Gong G, He Y, Concha L, Lebel C, Gross DW, Evans AC, et al. Mapping anatomical connectivity patterns of human cerebral cortex using in vivo diffusion tensor imaging tractography. Cereb Cortex 2009;19(3):524–36.
[49] Hagmann P, Kurant M, Gigandet X, Thiran P, Wedeen VJ, Meuli R, et al. Mapping human whole-brain structural networks with diffusion MRI. PloS One 2007;2(7):e597.
[50] Honey CJ, Kotter R, Breakspear M, Sporns O. Network structure of cerebral cortex shapes functional connectivity on multiple time scales. Proc Natl Acad Sci U S A 2007;104(24):10240–5.
[51] Johansen-Berg H, Behrens TE. Just pretty pictures? What diffusion tractography can add in clinical neuroscience. Curr Opin Neurol 2006;19(4):379–85.
[52] Gottwald B, Wilde B, Mihajlovic Z, Mehdorn HM. Evidence for distinct cognitive deficits after focal cerebellar lesions. J Neurol Neurosurg Psychiatry 2004;75(11):1524–31.
[53] Riva D, Giorgi C. The cerebellum contributes to higher functions during development: evidence from a series of children surgically treated for posterior fossa tumours. Brain 2000;123(Pt 5):1051–61.
[54] Scott RB, Stoodley CJ, Anslow P, Paul C, Stein JF, Sugden EM, et al. Lateralized cognitive deficits in children following cerebellar lesions. Dev Med Child Neurol 2001;43(10):685–91.
[55] Justus T. The cerebellum and English grammatical morphology: evidence from production, comprehension, and grammaticality judgments. J Cogn Neurosci 2004;16(7):1115–30.
[56] Leggio MG, Silveri MC, Petrosini L, Molinari M. Phonological grouping is specifically affected in cerebellar patients: a verbal fluency study. J Neurol Neurosurg Psychiatry 2000;69(1):102–6.
[57] Tedesco AM, Chiricozzi FR, Clausi S, Lupo M, Molinari M, Leggio MG. The cerebellar cognitive profile. Brain 2011;134(Pt 12):3672–86.
[58] Barrio-Arranz G, de Luis-Garcia R, Tristan-Vega A, Martin-Fernandez M, Aja-Fernandez S. Impact of MR acquisition parameters on DTI Scalar Indexes: a tractography based approach. PloS One 2015;10(10):e0137905.
[59] Yamamoto A, Miki Y, Urayama S, Fushimi Y, Okada T, Hanakawa T, et al. Diffusion tensor fiber tractography of the optic radiation: analysis with 6-, 12-, 40-, and 81-directional motion-probing gradients, a preliminary study. AJNR Am J Neuroradiol 2007;28(1):92–6.
[60] Wang S, Peterson DJ, Gatenby JC, Li W, Grabowski TJ, Madhyastha TM. Evaluation of field map and nonlinear registration methods for correction of susceptibility artifacts in diffusion MRI. Front Neuroinformatics 2017;11:17.

[61] Huang H, Ceritoglu C, Li X, Qiu A, Miller MI, van Zijl PC, et al. Correction of B0 susceptibility induced distortion in diffusion-weighted images using large-deformation diffeomorphic metric mapping. Magn Reson Imaging 2008;26(9):1294–302.
[62] Bammer R, Markl M, Barnett A, Acar B, Alley MT, Pelc NJ, et al. Analysis and generalized correction of the effect of spatial gradient field distortions in diffusion-weighted imaging. Magn Reson Med 2003;50(3):560–9.
[63] Chen NK, Wyrwicz AM. Optimized distortion correction technique for echo-planar imaging. Magn Reson Med 2001;45(3):525–8.
[64] EMd Souza, Costa ET, Castellano G. Phantoms for diffusion-weighted imaging and diffusion tensor imaging quality control: a review and new perspectives. Res Biomed Eng 2017;33(2):156–65.
[65] Jones DK. Diffusion MRI theory, methods, and applications. New York: Oxford University Press; 2011. [767 S. p.].